International Journal of Engineering, Mathematical and Physical Sciences
ISSN: 2517-9934
Vol:5, No:11, 2011

# A Robust TVD-WENO scheme for Conservation Laws

A. Abdalla and A. Kaltayev

***Abstract*—**The ultimate goal of this article is to develop a robust and accurate numerical method for solving hyperbolic conservation laws in one and two dimensions. A hybrid numerical method, coupling a cheap fourth order total variation diminishing (TVD) scheme [1] for smooth region and a Robust seventh-order weighted non-oscillatory (WENO) scheme [2] near discontinuities, is considered. High order multi-resolution analysis is used to detect the high gradients regions of the numerical solution in order to capture the shocks with the WENO scheme, while the smooth regions are computed with fourth order total variation diminishing (TVD). For time integration, we use the third order TVD Runge-Kutta scheme. The accuracy of the resulting hybrid high order scheme is comparable with these of WENO, but with significant decrease of the CPU cost. Numerical demonstrates that the proposed scheme is comparable to the high order WENO scheme and superior to the fourth order TVD scheme. Our scheme has the added advantage of simplicity and computational efficiency. Numerical tests are presented which show the robustness and effectiveness of the proposed scheme.

***Keywords*—**WENO scheme; TVD schemes; smoothness indicators; multi-resolution

## I. Introduction

THE present work is concerned with the numerical solution of the hyperbolic conservation laws. It is well known that the exact solutions to such equations may develop discontinuities in finite time, even when the initial condition is smooth, so that one needs to consider weak solutions. A successful method should compute such discontinuities with the correct position and without spurious oscillations and yet achieve a high order of accuracy in the regions of smoothness. Harten [1] introduced the total variation diminishing (TVD) schemes modified by many others. A fourth order total variation diminishing (TVD) scheme is presented in [1]. The main property of the TVD scheme is that it can be second order (or higher) and oscillations-free across discontinuities. Moreover, TVD schemes are very accurate in smooth parts. The disadvantage of the TVD schemes is that they avoid oscillations near discontinuities by locally reverting to first order of accuracy near discontinuities and extrema and are therefore unsuitable for applications involving long-time evolution of complex structures, such as in acoustic and compressible turbulence. The high order weighted essentially non-oscillatory (WENO) schemes are designed for this purpose. The WENO schemes were originally proposed by Liu et al [3], and have been improved by Jiang and Shu [4]. The motivation of this article is to combine the cheap fourth order TVD scheme [1] with the more expensive seventh order WENO scheme (k = 4) [2] to produce a fourth order accuracy inboth smooth parts and near discontinuities which is less expensive and therefore saves more CPU time. The expensive WENO scheme is used only near discontinuities and the fourth order TVD scheme is used in smooth parts. To distinguish between those regions we use a more efficient multi-resolution technique presented in [8]. The resulting scheme ensures that fluxes at grid points around discontinuities will always be computed by a WENO scheme; whereas smooth tendencies will not suffer any unnecessary extra damping because they will be treated by a TVD scheme. The rest of the article is organized as follows. Section 2 briefly reviews the WENO scheme [2]. In Section 3, we describe the fourth order TVD scheme [1]. The multi-resolution algorithm is discussed in Section 4. In Section 5, we present the hybrid scheme. Numerical results for one and two dimensional examples are presented in Section 6.

A. Abdalla is with department of mechanics, Al-Farabi Kazakh National University, Almaty, Kazakhstan (e-mail:amr.hassan1@hotmail.com).
A. Kaltayev is with department of mechanics, Al-Farabi Kazakh National University, Almaty, Kazakhstan

## II. The seven-order WENO scheme

Now, we will describe the WENO finite difference scheme for one dimensional scalar hyperbolic conservation law.

$$U_t + f(u)_x = 0, -\infty < x < \infty, t \geq 0, \; u(x,0) = u^0(x) \tag{1}$$

The semi-discrete finite difference formulation of (1) in a uniformly spaced grid is

$$d\left(u_j(t)\right)\Big/dt = -\left(f_{j+\frac{1}{2}} - f_{j-\frac{1}{2}}\right)\Big/\Delta x = L_j(u) \tag{2}$$

Where $\Delta x$ is the grid size, $u_j(t)$ is the solution within the stencil $I_j = \left[x_{j-\frac{1}{2}}, x_{j+\frac{1}{2}}\right]$, and the numerical flux

$$f_{j+\frac{1}{2}} = f\left(u_{j-r}, \ldots, u_{j+s}\right) \tag{3}$$

with r and s, integer parameters defining the set of values used for the computation of the flux $f(u)$.

In the current WENO schemes, the numerical solutions of (2) are advanced in time by means a TVD Runge-Kutta method [9] which will be discussed later. The key idea of a k-th order ENO scheme is to choose one "smoothest" stencil

$$s_r = \left\{x_{j-r}, \ldots, x_{j+s}\right\}, \text{ with } s = k - r - 1, \; r = 0 \ldots K - 1, \tag{4}$$

among the k candidate to avoid spurious oscillations near shocks. If the stencil $s_r$ happens to be chosen as the ENO interpolation stencil, then the k-th order ENO reconstruction of $f_{j+\frac{1}{2}}$ is: $p_r^j\left(x_{j+\frac{1}{2}}\right) = \hat{f}_{j+\frac{1}{2}} = \sum_{i=0}^{k-1} C_{ri} f_{j-r+i}$, (5)

where $C_{ri}$ is the constant coefficients obtained through Lagrangian interpolation process. This process is called the reconstruction step. WENO is an improved over ENO, for it

uses a convex combination of all available polynomials for a fixed k. This yields a (2k−1) order method at smooth parts of the solution. The flux $f_{j+1/2}$of WENO method is defined as

$$f_{j+\frac{1}{2}} = \sum_{i=0}^{k-1} w_r p_r^j\left(x_{j+\frac{1}{2}}\right), \tag{6}$$

The essentially non-oscillatory property is obtained by requiring that the weights $w_r$ reflect the relative smoothness of f:

$$w_r = \alpha_r / \alpha_0 + \alpha_1 + \ldots + \alpha_{k-1},\ r = 0,1,\ldots,\ k-1, \tag{7}$$

where $\alpha_r = d_r / (\varepsilon + IS_r)^2$ , and the parameter $\varepsilon$ is introduced to avoid the denominator to become zero. We take $\varepsilon = 10^{-6}$ in our numerical tests and $d_r$ are the optimal weight coefficients given by Balsara and Shu in [5]. $IS_r$is the smoothness measurement of the flux function on the r-th candidate stencil $S_r$.For the seventh-order WENO reconstruction (k=4), the corresponding smoothness indicators are given by

$$Is_r^k = \sum_{l=1}^{k-1} \beta_l \left[ u_i^{(l)}(i+r-k+1,\ldots,i+r)\Delta x^l \right] \tag{8}$$

where $u_i^{(l)}(i+r-k+1,\ldots,i+r)$ denotes the differencing approximation of $l$ th order derivative $u_i^{(l)}$ by using points $i+r-k+1,\ldots,i+r$. Because k points are used, the highest order approximation of $u_i^{(l)}$ is (k-l)-th order interpolation. The coefficients $\beta_l$ can affect the accuracy of the final scheme. For $u_i^{(l)}(i+r-k+1,\ldots,i+r)$, it can always be expressed as a linear combination of$(u_{i+r+1-n} - u_{i+r-n})$.

## III. TVD-Finite difference scheme

Under In this section, the fourth order explicit TVD schemes presented in [1] is reviewed. First let us consider the linear case $f(u) = au$ in (1) so that $f'(u) = a$ is a constant wave speed. The fourth order conservative TVD numerical fluxes introduced in [1] have the form:

$$f_{i+\frac{1}{2}} = \frac{1}{2}(au_i + au_{i+1}) - \frac{1}{2}|a|\Delta_{i+\frac{1}{2}}u + |a|\left\{A_0\Delta_{i+\frac{1}{2}}u + A_1\Delta_{i+L+\frac{1}{2}}u\right\}\varnothing_i + |a|A_2\Delta_{i+M+\frac{1}{2}}u\varnothing_{i+M}. \tag{9}$$

where L = −1, M = 1 for c > 0 and L = 1, M = −1 for c < 0. Here $c = a\Delta t/\Delta x$ is the Courant number, t is the time step, and $\Delta_{i+\frac{1}{2}} u_j = u_{j+1} - u_j$, where

$$\begin{aligned} A_0 &= \tfrac{1}{2} - \left(7|c|/12\right) + \left(|c^3|/12\right), \\ A_1 &= \tfrac{1}{12} + \left(|c|/24\right) - \left(|c^2|/12\right) - \left(|c^3|/24\right), \\ A_2 &= -\tfrac{1}{12} + \left(|c|/24\right) + \left(|c^2|/12\right) - \left(|c^3|/24\right). \end{aligned} \tag{10}$$

Here $\varnothing_i$ and $\varnothing_{i+M}$are flux limiter functions defined by

$$\varnothing_i = \begin{cases} (1-|c|)\theta_i / \gamma(A_1\theta_i + A_0 - A_2) & for\ 0 \le \theta_i \le \theta^L \\ 1 & for\ \theta^L \le \theta_i \le \theta^R \\ 1 - |c| + \gamma A_2 \varnothing_i + M/\theta_i^* / \gamma(A_1\theta_i + A_0) & for\ \theta_i > \theta^R \\ 0 & for\ \theta_i < 0 \end{cases} \tag{11a}$$

$$\varnothing_{i+M} = \begin{cases} \gamma\theta_{i+M} & for\ 0 \le \theta_{i+M} < 0.5 \\ 1 & for\ \theta_{i+M} > 0.5 \\ 0 & for\ \theta_i = 0 \end{cases} \tag{11b}$$

Where

$$\theta^L = \frac{\gamma(A_0 - A_2)}{1 - |c| - \gamma A_1},\quad \theta^R = \frac{1 - |c| - \gamma\left(A_0 - A_2\varnothing_{i+M}/\theta_i^*\right)}{\gamma A_1},$$

here $\theta_i$ is called the local flow parameter and is defined by

$$\theta_i = \Delta_{i+L+\frac{1}{2}}u / \Delta_{i+\frac{1}{2}}u, \tag{12a}$$

and $\theta_j^*$is called the upwind-downward flow parameter and is given by

$$\theta_i^* = \Delta_{i+L+\frac{1}{2}}u / \Delta_{i+M+\frac{1}{2}}u, \tag{12b}$$

and $\gamma$ is defined by

$$\gamma = \begin{cases} 1 - |c| & for\ 0 \le |c| < 1/2 \\ |c| & for\ 1/2 \le |c| \le 1 \end{cases}. \tag{13}$$

For nonlinear scalar problems $a = a(u)$, we define the wave speed

$$a_{i+\frac{1}{2}} = \begin{cases} \Delta_{i+\frac{1}{2}}f / \Delta_{i+\frac{1}{2}}u,\ \Delta_{i+\frac{1}{2}}u \ne 0 \\ \partial f / \partial u|_{u_i},\quad \Delta_{i+\frac{1}{2}}u = 0 \end{cases}. \tag{14}$$

Now we redefine $\theta_i$ in (12a) as

$$\theta_i = \left|a_{i+L+\frac{1}{2}}\right| \Delta_{i+L+\frac{1}{2}}u / \left|a_{i+\frac{1}{2}}\right| \Delta_{i+\frac{1}{2}}u. \tag{15}$$

here c is replaced by $c_{i+\frac{1}{2}} = a_{i+\frac{1}{2}}\Delta t/\Delta x$.

The numerical flux (9) takes the form

$$f_{i+\frac{1}{2}} = \frac{1}{2}(f_i + f_{i+1}) - \frac{1}{2}\left|a_{i+\frac{1}{2}}\right|\Delta_{i+\frac{1}{2}}u + \left|a_{i+\frac{1}{2}}\right|\left\{A_0\Delta_{i+\frac{1}{2}}u + A_1\Delta_{i+L+\frac{1}{2}}u\right\}\varnothing_i + \left|a_{i+\frac{1}{2}}\right|A_2\Delta_{i+M+\frac{1}{2}}u\varnothing_{i+M} \tag{16}$$

The flux limiter becomes the same (11) with replacing c by $c_{j+1/2}$.With stability condition CFL ≤ 1, here CFL denotes the maximum Courant number over all cells at a given time step.

## IV. Multi-Resolution Analysis

The successful implementation of the Hybrid method depends on the ability to obtain accurate information on the smoothness of a function. In this work, we employ the Multi-Resolution (MR) algorithms by Harten [7, 10] to detect the smooth and rough parts of the numerical solution. The general idea is to generate a coarser grid of averages of the point values of a function and measure the differences (MR coefficients) $d_k^j$ between the interpolated values from this sub-grid and the point values them-selves. A tolerance parameter MR is chosen in order to classify as smooth those parts of the function that can be well interpolated by the averaged function and as rough those where the differences $d_k^j$ are larger than the parameter MR. We shall see that the order of interpolation is relevant and the ratio between $d_k^j$ of distinct orders may also be taken as an indication of smoothness.

*Consider a set of dyadic grids on the form*

$$V^j = \left\{ x_k^j \in R : x_k^j = 2^{-j} k, k \in Z \right\},\ j \in Z \tag{17}$$

where j identifies the resolution level and k the spatial location, as illustrated in Fig. 4. Assume that the solution is known on grid $V^j$ for $J_{min} \le j \le J_{max}$ and we want to extend it to the finer grid $V^{j+1}$. Values on the even-numbered grid points are known from the corresponding values on the lower resolution grid:

$$u_{2k}^{j+1} = u_k^j, \tag{18}$$

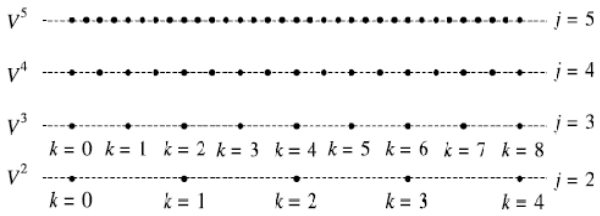


Fig. 1 Example of points in a dyadic grid

whereas the function values in the odd numbered grid points in $V^{j+1}$ are computed using a suitable interpolation scheme, based on the known even-numbered grid points. The interpolative error coefficient (or multi-resolution coefficient), $d_k^j$ is defined as the difference between the interpolated value, $I^j\left(u_{2k+1}^{j+1}\right)$, and the real one, $u_{2k+1}^{j+1}$,

$$d_k^j = \left| u_{2k+1}^{j+1} - I^j\left(u_{2k+1}^{j+1}\right) \right| / u_{ref} \tag{19}$$

$u_{ref}$ is a reference value of the dependent variable such that,

$$u_{ref} = max\left( \left| u_{2k+1}^{j+1} \right| \right), \quad k = 0,1,\ldots,2^j, \tag{20}$$

The calculation of the interpolated values is illustrated for the case of odd numbered grid point:

a- Calculate the face velocity

$$a_{k+\frac{1}{2}} = \left(a_k^j + a_{k+1}^j\right)/2 \cdot \tag{21}$$

b- Calculate the normalized face value $\widehat{u}_{j+\frac{1}{2}}$, using the SMART high resolution scheme [6], the normalized face value is given by

$$\widehat{u}_{k+\frac{1}{2}} = \begin{cases} \max\left\{ \left( \dfrac{u_k^j - u_{k-1}^j}{u_{k+1}^j - u_{k-1}^j} \right), \min\left( 3\dfrac{u_k^j - u_{k-1}^j}{u_{k+1}^j - u_{k-1}^j}, \dfrac{3}{4}\dfrac{u_k^j - u_{k-1}^j}{u_{k+1}^j - u_{k-1}^j} + \dfrac{3}{8}, 1 \right) \right\}, & \text{if } a_{k+\frac{1}{2}} \ge 0 \\ \max\left\{ \left( \dfrac{u_{k+1}^j - u_{k+2}^j}{u_k^j - u_{k+2}^j} \right), \min\left( 3\dfrac{u_{k+1}^j - u_{k+2}^j}{u_k^j - u_{k+2}^j}, \dfrac{3}{4}\dfrac{u_{k+1}^j - u_{k+2}^j}{u_k^j - u_{k+2}^j} + \dfrac{3}{8}, 1 \right) \right\}, & \text{if } a_{k+\frac{1}{2}} < 0 \end{cases} \tag{22}$$

c- Calculate the interpolated value:

$$I^j\left(u_{2k+1}^{j+1}\right) = \begin{cases} u_{k-1}^j + \tilde{u}_{k+\frac{1}{2}}^j \left( u_{k+1}^j - u_{k-1}^j \right), & if\ a_{k+\frac{1}{2}} \ge 0 \\ u_{k+2}^j + \tilde{u}_{k+\frac{1}{2}}^j \left( u_k^j - u_{k+2}^j \right), & if\ a_{k+\frac{1}{2}} < 0 \end{cases} \tag{23}$$

The maximum level of resolution is specified by the user so that grid coalescence is avoided in problematic regions (typically in this work we used $J_{max} = 12$). The user also supplies the minimum level of resolution, and all the grid points pertaining to this level of resolution are always conserved throughout the computations (typically in this work we set $J_{max} = 4$).

## V. Hybrid Method

In this section, we describe the hybrid TVD-WENO scheme. It is defined as a grid-based adaptive method in which the choice of the numerical scheme is determined by the smoothness of the solution at each grid point which is measured by the multi-resolution procedure mentioned in Section 5. The fourth -order TVD scheme is used at those grid points where the solution is flagged as smooth in lieu of the standard high order WENO scheme. The hybrid scheme is summarized in the following steps:

(1) Assume that the function values $u_k^j$ in the grid $V^j$ at time $t = t_l$, compute the multi-resolution coefficients $d_k^j$ for $J_{min} \le j \le J_{max}$ from Equation (19).

(2) A grid point is flagged as non-smooth when $\left| d_k^j \right| > \varepsilon$ ($\varepsilon$ is a tolerance parameter defined by the user): $flag_i = \begin{cases} 1, if \left| d_k^j \right| > \varepsilon \\ 0, otherwise \end{cases}$

(3) Once the flags are set, a number of neighboring points around each flagged points $x_i$, depending on the number of the ghost points needed for a given difference scheme and WENO scheme, are also flagged to 1. In particular, if $n_f$ and $n_w$ are the orders of the TVD-difference and WENO schemes respectively, the number of ghost points required by the TVD-difference and WENO schemes are $n_f/2$ and $\left(n_w + 1\right)/2$, respectively. At any given point, say $x_i$, flagged as non-smooth, its $r = \max\left(n_f/2, \left(n_w + 1\right)/2\right)$ neighboring points $\{x_{i-r}, \ldots, x_i, \ldots, x_{i+r}\}$ will also be designated as non-smooth, that is, $\{flag_j = 1,\ j = i - r, \ldots, i + r\}$. This procedure avoids computing the derivative of the solution by the difference scheme using non-smooth functional values. Furthermore, the same WENO flag will be used at the Runge-Kutta stages and will be updated at the next time step.

(4) For the grid points flagged zero (smooth), we compute $u_j^{n+1}$ by solving the ODE (2) using the numerical flux $f_{j+1/2}$ (9) and the Runge–Kutta scheme.

(5) For the grid points designated as non-smooth we compute $u_j^{n+1}$ by WENO scheme.

## VI. Numerical Results

In this section, two examples are presented to illustrate the efficiency and robustness of the proposed scheme. For all tests we use a uniform mesh; N denotes the number of cells and the exact solution is shown by the solid line and the numerical solution by symbols.

*Example 1 (Burgers' equation)*

This example considers the numerical solution of the inviscid Burgers' equation

$$u_t + \left(u^2/2\right)_x = 0 \quad , \quad u(x,0) = \begin{cases} -1, & |x| \geq 0.5 \\ 2, & |x| < 0.5 \end{cases} \tag{24}$$

The breakdown of the initial discontinuity results in a shock wave with speed 0.5 and a rarefaction with a sonic point at x =0.5. The exact solution consists of rarefaction wave (left) and shock wave (right). At $t=⅔$ the rarefaction hits the shock and then the solution has a rarefaction wave only. The numerical solution is displayed at t =0.4 (before collision of the head of the rarefaction with the shock) and t =1.1 (after collision). Results are shown in Figure 2, with $2^6+1$ grid points,Multi-resolution tolerance $\varepsilon = 10^{-3}$ and CFL=0.45. Note that the hybrid method reproduces the exact solution.

*Example 2 (Shock reflection problem)*

Now we test our hybrid scheme on the system of Euler equations of gas dynamics

$$U_t + F(U)_x = 0 \tag{25}$$

where $U = (\rho, \rho u, E)^T$ and $F(U) = \left(\rho u, \rho u^2 + P, u(E+P)\right)^T$, where $\rho$ is the density, $u$ is the velocity, $P$ is the pressure, $E = \rho e + \left(\rho u^2\right)/2$ is the total energy (sum of internal energy and kinetic energy); $e$ is the specific internal energy $e = P/\rho(\gamma - 1)$ and $\gamma$ is the ratio of specific heats.

We consider the test problem concerning shock reflection in one dimension $0 \leq x \leq 1$, governed by Euler equations of monatomic gas $\gamma = ⅔$ with initial data [11]: $\rho = \rho_0,\ u = u_0,\ e = e_0$

This represents a gas of constant density and pressure moving towards $x = 0$. The boundary $x = 0$ is a rigid wall and exact solution describes shock reflection from the wall. The gas is brought to rest at $x = 0$, $\rho_0 = 1,\ u_0 = 1,\ P_0 = 3,$ and $e(x,t)$ is chosen such that the pressure jump across the shock equals 2, i.e. $e_0 = 4.5$. Figure 3 illustrates the results at t =0.15 and mesh size of $2^7+1$ grid points with multi-resolution tolerance $\varepsilon = 10^{-3}$ and CFL=0.45. We observe that the hybrid scheme resolves the discontinuity exactly.

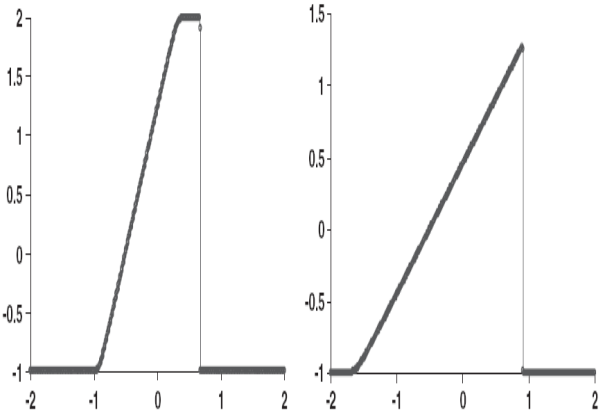


Fig. 2 Solution of Example 1 using the hybrid scheme at t =0.4 (left) and t =1.1 (right).

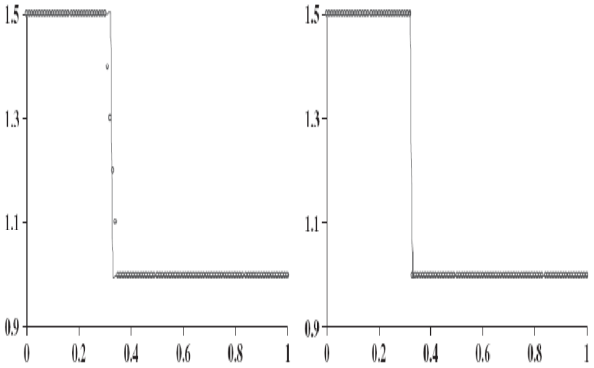


Fig. 3 Solution of Example 2 using third-order scheme (left) and hybrid scheme (right) at t =0.15

## VII. Conclusions

We have presented an efficient, accurate and high-resolution hybrid scheme. In this scheme we use the fourth-order TVD scheme in the smooth region and the seven-order WENO scheme near discontinuities. The numerical solution is advanced in time by the third-order Runge–Kutta method. The main advantages of the scheme are reduction of CPU time and improvement in overall accuracy over the classical TVD schemes. This is due to the use of more accurate seven-order WENO scheme near discontinuities and high-order TVD scheme in the smooth region. We use an efficient multi-resolution technique to detect the discontinuities. This scheme is tested and validated by solving one- and two-dimensional problems.

## References

[1] J. Shi and E. F. Toro, "Fully discrete high resolution schemes for hyperbolic conservation laws," Int. J. Num. Method Fluids., vol. 23, PP. 241–269, 1996.

[2] Y. Shen and G. Zhay, "A Robust Seventh-order WENO Scheme and Its Applications" AIAA Paper 2008-0757.

[3] X.D. Liu, S. Osher, and T. Chan, "Weighted essentially non-oscillatory schemes" J. Comput. Phys., vol. 126, pp. 200-212, 1994.

[4] G.S. Jiang, and C.W. Shu,"Efficient implementation of weighted ENO schemes" J. Comput. Phys., vol. 126, pp. 202-228, 1996.

[5] D.S. Balsara and C.-W. Shu, "Monotonicity Preserving weighted essentially non-oscillatory schemes with increasingly high order of accuracy," J.Comput.Phys., vol. 160, pp. 405-452, 2000.

[6] Z.F. Xu and C.-W. Shu, "Anti-diffusive flux corrections for high order finite difference WENO schemes," J.Comput.Phys., vol. 205, pp. 458-485, 2005.

[7] A. Harten, "Adaptive multi-resolution schemes for shock computations," Comput Phys., vol. 115, PP. 319–338, 1994.

[8] M. A. Alves, P. Cruz, A. Mendes, F. D. Magalhaes, F. T. Pinho, and P. J. Oliveira, "Adaptive multi-resolution approach for solution of hyperbolic PDEs," Comput Methods Appl. Mech Eng., vol. 191,PP. 3909–3928, 2002.

[9] S. Gotlieb and C. W. Shu, "Total variation diminishing Runge-Kutta schemes," Math Comp., vol. 67, PP. 73–85, 1998.

[10] A. Harten, High resolution schemes for hyperbolic conservation laws, J Comput Phys., vol. 49, PP. 357–393, 1983.

[11] Glaister P. "An approximate linearized Riemann solver for Euler equations for real gases". Journal of Computational Physics., vol. 74, PP. 382–408, 1988.